Supporting Material for "Cross-validating FRAP and FCS to Quantify the Impact of Photobleaching on In Vivo Binding Estimates"

Timothy J. Stasevich[1,*], Florian Mueller[1,*], Ariel Michelman-Ribeiro[1,2], Tilman Rosales[3], Jay R. Knutson[3], and James G. McNally[1,†]

[1]National Cancer Institute, US National Institutes of Health, Bethesda, MD 20892, USA
[2]present address - Semiconductor Electronics Division, Electronics and Electrical Engineering Laboratory, National Institute of Standards and Technology. Gaithersburg, MD 20899, USA.
[3]Laboratory of Molecular Biophysics, National Heart, Blood and Lung Institute, National Institutes of Health. Bethesda, MD 20892, USA.

[*]These authors contributed equally to this work.

[†]Corresponding author: Phone: (301) 402-0209
E-mail: mcnallyj@exchange.nih.gov
FAX: (301) 496-4951

Cells

Cells were grown in Labtek II microscope chambers (Nalgene, Rochester, NY) in Dulbecco's modified Eagle's medium (DMEM) supplemented with 10% fetal bovine serum, 1% glutamine, and 0.5% penicillin-streptomycin. Cells were routinely kept in a 37°C incubator with 5% CO_2. Transient transfections of the VBP-B-ZIP-GFP plasmid (0.5 μg/ml) were done in Opti-mem medium (Invitrogen, Carlsbad, CA) using Lipofectamine 2000 reagent (Invitrogen) (1.5 μl/ml) according to the manufacturer's instructions.

FCS calibration

The two-photon excitation volume was calibrated by measuring the diffusion of Alexa 488 (196 $\mu m^2/s$ (1)), rhodamine 110 (270-300 $\mu m^2/s$ (1)) (Invitrogen, Carlsbad, CA), and unconjugated GFP (82 ± 4 $\mu m^2/s$, see Table S1 below) in water and/or PBS at 25°C (Biovision, Mountain View, CA) using a wavelength of 970 nm, resulting in $w_r = 0.35$ μm and $w_z = 1.5$ μm.

The one-photon excitation volume was calibrated by measuring the diffusion of Rhodamine 6G (280-300 $\mu m^2/s$ (2,3) in water at 25°C using a wavelength of 488 nm, resulting in $w_r = 0.19$ μm and $w_z = 0.95$ μm. All cells were imaged at 37 ºC using an objective heater (Bioptechs Inc., Butler, PA) for two-photon FCS and a heating unit (PeCon, Erbach, Germany) for one-photon FCS.

TICS (Temporal Image Correlation Spectroscopy) calibration

The TICS measurement volume was calibrated by first measuring the PSF (Point Spread Function) of the Zeiss LSM 5 LIVE with 105 nm diameter fluorescent beads mounted onto a glass coverslip with Aquamount (Thermo Scientific, Waltham, MA). Image stacks of these beads were reasonably fit with a 3D Gaussian, with $w_x = 0.3 \pm 0.13$ μm, $w_y = 0.25 \pm 0.09$ μm, and $w_z = 0.90 \pm 0.20$ μm (Fig. S8), consistent with earlier measurements using the same microscope (4). The accuracy of this PSF was tested by using it to estimate the diffusion coefficient of fluorescent beads diffusing in solution. Correct estimates were obtained for both 105 nm and 210 nm beads with $w_x = 0.38$ μm, $w_y = 0.27$ μm, and $w_z = 1.1$ μm (Figs. S6A and B). These values were used to describe the PSF in subsequent fits.

Common reaction-diffusion model for FRAP, FCS, and TICS

We fit our data with a reaction-diffusion model in which molecules are assumed to freely diffuse with diffusion coefficient D_f and bind and unbind to homogeneously distributed immobile binding sites with association and dissociation rates k_{on}^* and k_{off}. If $f(\vec{r},t)$ is the concentration of unbound, freely diffusing molecules and $c(\vec{r},t)$ is the concentration of bound molecule, then $f(\vec{r},t)$ and $c(\vec{r},t)$ satisfy the following set of coupled differential equations:

$$\begin{aligned} \frac{\partial f}{\partial t} &= D_f \nabla^2 f - k_{on}^* f + k_{off} c \\ \frac{\partial c}{\partial t} &= k_{on}^* f - k_{off} c \end{aligned} \tag{1.1}$$

We assume the system is at equilibrium, so $f(\vec{r},t)$ and $c(\vec{r},t)$ have achieved steady-state values: $F_{eq} = k_{off}/(k_{on}^* + k_{off})$ and $B \equiv C_{eq} = k_{on}^*/(k_{on}^* + k_{off})$.

FRAP solution and fitting equations

For FRAP, we model the nucleus as a sphere with radius R_N and assume the intentional photobleach is uniform along the axial direction of the sphere, so the system is cylindrically symmetric and can therefore be fully described in 2D rather than 3D. In this case, $\vec{r}$ is replaced by r, the radial distance from the axial profile. The initial conditions are specified by the radial distribution of total fluorescence $I_o(r)$ just after the intentional FRAP photobleach. This can be experimentally fit from the first post-bleach frame of a FRAP movie. For our data we find $I_o(r)$ is well described by a constant function with Gaussian flanks:

$$I_0(r) = \begin{cases} \theta & \text{for } r \le r_c \\ 1-(1-\theta)\exp\left(-\dfrac{(r-r_c)^2}{2\sigma^2}\right) & \text{for } r > r_c, \end{cases} \tag{1.2}$$

We assume a sufficiently fast intentional photobleach that similarly alters the fluorescence of both the bound and freely diffusing molecules, so $f(r,0) = F_{eq} I_0(r)$ and $c(r,0) = C_{eq} I_0(r)$. We also assume the nucleus is sufficiently large so there is no flux in fluorescence at the nuclear membrane $r = R_N$.

With these assumptions, the FRAP recovery $frap(r,t)$ can be written as a series expansion (5):

$$\begin{aligned} frap(r,t) &= f(r,t) + c(r,t) \\ &= \sum_{k=0}^{\infty} \left[(U_k + W_k)\exp(-(w_k + v_k)t) + (V_k + X_k)\exp(-(w_k - v_k)t) \right] J_0(\alpha_k r), \end{aligned} \tag{1.3}$$

where J_0 are Bessel functions and the constants are defined as

$$w_k = \frac{1}{2}\left(D_f \alpha_k^2 + k_{on}^* + k_{off}\right) \quad \text{and} \quad v_k = \sqrt{\frac{1}{4}\left(D_f \alpha_k^2 + k_{on}^* + k_{off}\right)^2 - k_{off} D_f \alpha_k^2}. \tag{1.4}$$

$$\begin{aligned} U_k &= \frac{1}{-2k_{off} v_k}[(-w_k - v_k + k_{off})(w_k - v_k)] \frac{2F_{eq}}{R_N^2 J_0^2(\chi_k)} \int_0^{R_N} I_0(r)\, J_0(\alpha_k r)\, r\, dr \\ V_k &= \frac{1}{2k_{off} v_k}[(-w_k + v_k + k_{off})(w_k + v_k)] \frac{2F_{eq}}{R_N^2 J_0^2(\chi_k)} \int_0^{R_N} I_0(r)\, J_0(\alpha_k r)\, r\, dr \end{aligned} \tag{1.5}$$

$$W_k = U_k \frac{k_{on}^*}{-(w_k + v_k) + k_{off}}, \quad X_k = V_k \frac{k_{on}^*}{-(w_k - v_k) + k_{off}}. \tag{1.6}$$

Here χ_k is the k^{th} zero of the Bessel function of the first kind and $\alpha_k = \chi_k / R_N$. For typical fitting of FRAP recovery curves, the sum in Eq. (1.3) is truncated at 500 terms. As described in the main text, we experimentally measure *frap(r,t)* by radially averaging the fluorescence in concentric rings centered on the bleach spot. When these data are normalized by the pre-bleach value and corrected for photobleaching, they can be directly fit with Eq. (1.3).

FCS/TICS solution and fitting equations

For FCS/TICS, we first note that Eq. (1.1) for *f* and *c* is also satisfied by the equilibrium concentration fluctuations $\delta f \equiv f - F_{eq}$ and $\delta c \equiv c - C_{eq}$. If we assume the observation

volume is approximately a 3D Gaussian, then the fluctuations are described by the following autocorrelation function, *G(t)* (6):

$$G(t) = \frac{w_x w_y w_z}{8N(2\pi\mu)^{3/2}} \int \Gamma(\vec{q}) \Omega(\vec{q},t) d^3\vec{q}, \tag{1.7}$$

where *N* is the number of fluorescent molecules in the observation volume, $\mu = 1,2$ for one or two photon excitation, w_x, w_y, and w_z are the widths of the observation volume, and $\vec{q} = (q_x, q_y, q_z)$ is the Fourier transform variable. The term $\Gamma(\vec{q})$ accounts for the illumination profile:

$$\Gamma(\vec{q}) = e^{-\frac{w_x^2}{4\mu}q_x^2 - \frac{w_y^2}{4\mu}q_y^2 - \frac{w_z^2}{4\mu}q_z^2}, \tag{1.8}$$

while the term $\Omega(\vec{q},t)$ accounts for the diffusion and chemical kinetics:

$$\Omega(\vec{q},t) = \frac{1}{2}\left[e^{\lambda_1 t}(1-\phi) + e^{\lambda_2 t}(1+\phi)\right], \tag{1.9}$$

with the λ's given by:

$$\begin{aligned} \lambda_1 &= \frac{1}{2}\left(-q^2 D_f - k_{off} - k_{on}^* - \sqrt{\alpha}\right) \\ \lambda_2 &= \frac{1}{2}\left(-q^2 D_f - k_{off} - k_{on}^* + \sqrt{\alpha}\right) \end{aligned}, \tag{1.10}$$

ϕ given by:

$$\phi = \frac{k_{on}^* + k_{off}}{\sqrt{\alpha}} + \frac{k_{on}^* - k_{off}}{k_{on}^* + k_{off}} \frac{q^2 D_f}{\sqrt{\alpha}}, \tag{1.11}$$

and $q^2 = q_x^2 + q_y^2 + q_z^2$ and $\alpha = \left(q^2 D_f + k_{on}^* + k_{off}\right)^2 - 4q^2 D_f k_{off}$.

The equations above describe the general solution, but the GFP-GR auto-correlation can also be fit by a simplified equation that is valid when the average time $\tau_D = \langle w^2 \rangle / (4\mu D t)$ to diffuse across the lateral portion of the focal volume is much shorter than the average time to associate with a binding site $1/k_{on}^*$ (i.e. $\tau_D << 1/k_{on}^*$). Here the $\langle\ \rangle$ brackets denote an average in the lateral directions *x* and *y*. We refer to this regime as "reaction-dominant" (6). In this case, the autocorrelation function can be decomposed into a sum of two parts, the first part from the freely diffusing molecules, the second part from the bound molecules:

$$G(t) = \frac{1}{2^{3/2} N}\left(F_{eq}\left(1+\frac{4\mu D t}{{\omega_x}^2}\right)^{-1/2}\left(1+\frac{4\mu D t}{{\omega_y}^2}\right)^{-1/2}\left(1+\frac{4\mu D t}{{\omega_z}^2}\right)^{-1/2} + C_{eq} e^{-k_{off} t}\right). \quad (1.12)$$

Calculation of the theoretical diffusion constant of fluorescent beads and unconjugated GFP

We measured the diffusion coefficient of fluorescent beads and unconjugated GFP in solution to calibrate and test our FCS and TICS setups. We compared the measurements to theoretical values calculated from the Stokes–Einstein equation $D = k_B T / 6\pi\eta\sigma$, where k_B is the Boltzmann constant, T is the absolute temperature, η is the viscosity, and σ is the hydrodynamic radius (7). Viscosity values were extrapolated from data in the Handbook of Chemistry and Physics (8). For the hydrodynamic radius of unconjugated GFP we used a value of 2.82 nm (9). The calculated theoretical diffusion coefficients are summarized in Table S1.

Experiment	Tracer	Solution	T (°C)	η	σ (nm)	D ($\mu m^2/s$)
1P/2P-FCS	GFP	100% PBS	23 ± 2	0.94 ± 0.04	2.82	82 ± 4
	GFP	90 ± 2% glycerol	23 ± 2	186 ± 81	2.82	0.43 ± 0.16
TICS	200nm bead	100% H_20	37 ± 2	0.69 ± 0.03	100	3.28 ± 0.15
	100nm bead	100% H_20	37 ± 2	0.69 ± 0.03	50	6.56 ± 0.3
	GFP	90 ± 2% glycerol	37 ± 2	75 ± 30	2.82	1.1 ± 0.4

Table S1

Converting from diffusion coefficients to focal volume residence times

In Figs. 4B and 5B of the main text we show that the fitted FCS focal volume residence time τ_{FV} can decrease as the laser power increases, indicative of cryptic photobleaching. We focused on τ_{FV} in these figures rather than the diffusion coefficient *D* to make the analogy with Fig. 4C, which shows fitted binding residence times t_r can also decrease with increasing laser power.

To calculate τ_{FV} in terms of *D* (from Table S1) we note that the probability $P(\vec{r},t)$ a molecule with diffusion coefficient *D* has diffused a distance $\vec{r}$ in time *t* is (7):

$$P(\vec{r},t) = \frac{1}{(4\pi D t)^{3/2}} e^{-r^2/(4Dt)}. \quad (1.13)$$

If we assume the particle was initially at the center of the two-photon FCS focal volume V_f, then the probability *P(t)* that the molecule is still in the focal volume a time *t* later is

$$
\begin{aligned}
P(t) &= \iiint_{V_f} d\vec{r}\,P(\vec{r},t) \\
&= \int_{-w_z}^{w_z}\int_{-w_y}^{w_y}\int_{-w_x}^{w_x} \frac{d\vec{r}}{(4\pi Dt)^{3/2}} e^{-r^2/(4Dt)} \qquad (1.14) \\
&= Erf\left[\frac{w_x}{2\sqrt{Dt}}\right] Erf\left[\frac{w_y}{2\sqrt{Dt}}\right] Erf\left[\frac{w_z}{2\sqrt{Dt}}\right],
\end{aligned}
$$

where w_x, w_y, and w_z are the dimensions of the two-photon FCS focal volume and *Erf* is the error function. To make the analogy to a binding residence time, we set this probability equal to $e^{-t/\tau_{FV}}$:

$$P(t) = e^{-t/\tau_{FV}} \qquad (1.15)$$

Letting $t = \tau_{FV}$ yields a transcendental equation that we numerically solve to find the focal volume residence time τ_{FV}:

$$Erf\left[\frac{w_x}{2\sqrt{D\tau_{FV}}}\right] Erf\left[\frac{w_y}{2\sqrt{D\tau_{FV}}}\right] Erf\left[\frac{w_z}{2\sqrt{D\tau_{FV}}}\right] = e^{-1} \qquad (1.16)$$

For Figs. 4B and 5B, we used $D = 0.43 \pm 0.16$ μm^2/s (see Table S1) in Eq. (1.16) to calculate theoretical values for $\tau_{FV} = 0.23 \pm 0.09$ s for two-photon FCS (w_r=0.35 μm and w_z=1.5 μm) and $\tau_{FV} = 0.058 \pm 0.024$ s for one-photon FCS (w_r=0.19 μm and w_z=0.95 μm). For Fig. S5 we used $D = 82 \pm 4$ μm^2/s in Eq. (1.16) to calculate a theoretical value for $\tau_{FV} = 0.001 \pm 0.0001$ s.

Reference List

1. Pristinski,D., V.Kozlovskaya, and S.A.Sukhishvili. 2005. Fluorescence correlation spectroscopy studies of diffusion of a weak polyelectrolyte in aqueous solutions. *J Chem Phys* 122:14907.

2. Berland,K.M. 2004. Detection of specific DNA sequences using dual-color two-photon fluorescence correlation spectroscopy. *J Biotechnol* 108:127-136.

3. Magde,D., E.L.Elson, and W.W.Webb. 1974. Fluorescence correlation spectroscopy. II. An experimental realization. *Biopolymers* 13:29-61.

4. Wolleschensky,R., B.Zimmermann, and M.Kempe. 2006. High-speed confocal fluorescence imaging with a novel line scanning microscope. *Journal of Biomedical Optics* 11.

5. Mueller,F., P.Wach, and J.G.McNally. 2008. Evidence for a common mode of transcription factor interaction with chromatin as revealed by improved quantitative fluorescence recovery after photobleaching. *Biophysical Journal* 94:3323-3339.

6. Michelman-Ribeiro,A., D.Mazza, T.Rosales, T.J.Stasevich, H.Boukari, V.Rishi, C.Vinson, J.R.Knutson, and J.G.McNally. 2009. Direct Measurement of Association and Dissociation Rates of DNA Binding in Live Cells by Fluorescence Correlation Spectroscopy. *Biophysical Journal* 97:337-346.

7. Berg H.C. 1993. Random Walks in Biology. Princeton University Press.

8. Hogman C.D., Wheast R.C., Shankland R.S., and Selby S.M. 1961. Handbook of Chemistry and Physics. The Chemical Rubber Publishing Co..

9. Terry,B.R., E.K.Matthews, and J.Haseloff. 1995. Molecular Characterization of Recombinant Green Fluorescent Protein by Fluorescence Correlation Microscopy. *Biochemical and Biophysical Research Communications* 217:21-27.

10. Mikuni,S., M.Tamura, and M.Kinjo. 2007. Analysis of intranuclear binding process of glucocorticoid receptor using fluorescence correlation spectroscopy. *Febs Letters* 581:389-393.

11. Petrasek,Z. and P.Schwille. 2008. Precise measurement of diffusion coefficients using scanning fluorescence correlation spectroscopy. *Biophys J* 94:1437-1448.

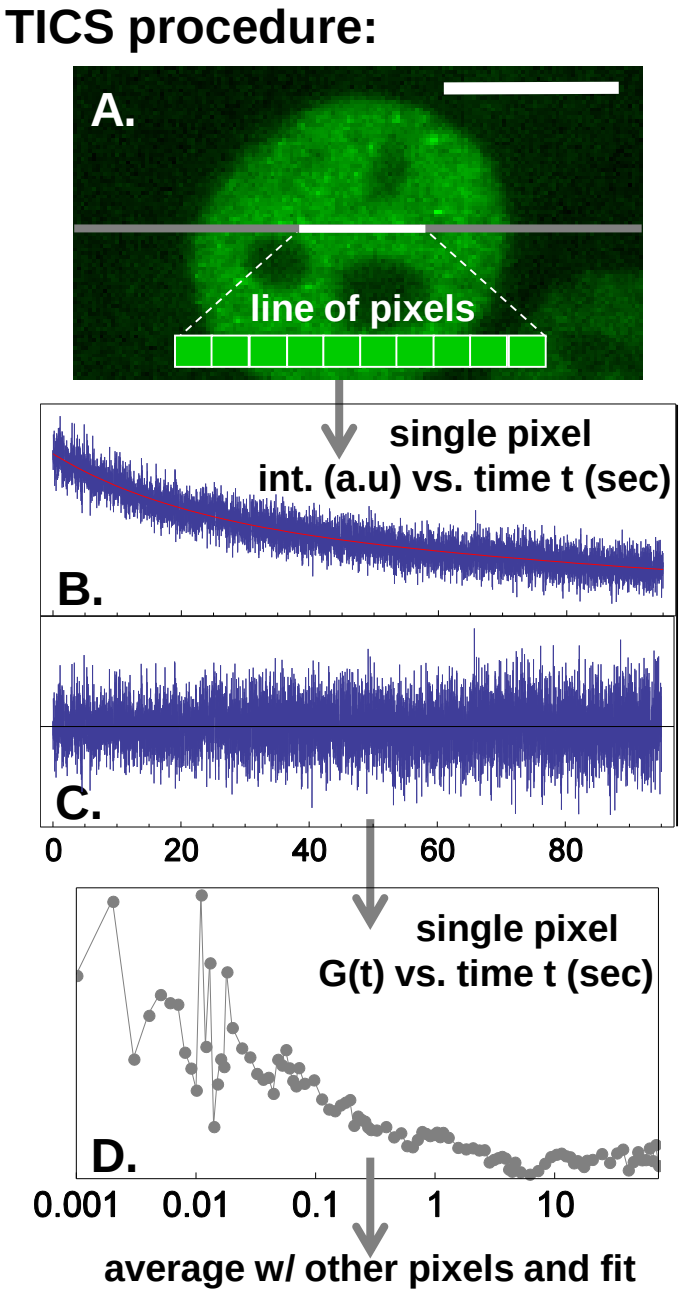

FIGURE S1. The TICS (Temporal Image Correlation Spectroscopy) procedure: (A) A line passing through the center of a fluorescently homogeneous region of a cell was imaged repeatedly at up to 4000 Hz. **(B)** The intensity of each pixel decays exponentially with time due to photobleaching, unlike in two-photon FCS where a much smaller volume is illuminated and so the photobleaching is cryptic. **(C)** When the data are corrected for photobleaching, fluctuations are about a non-decaying mean. **(D)** The autocorrelation G(t) of data from each pixel can then be calculated. Averages of these individual G(t) are used for fitting.

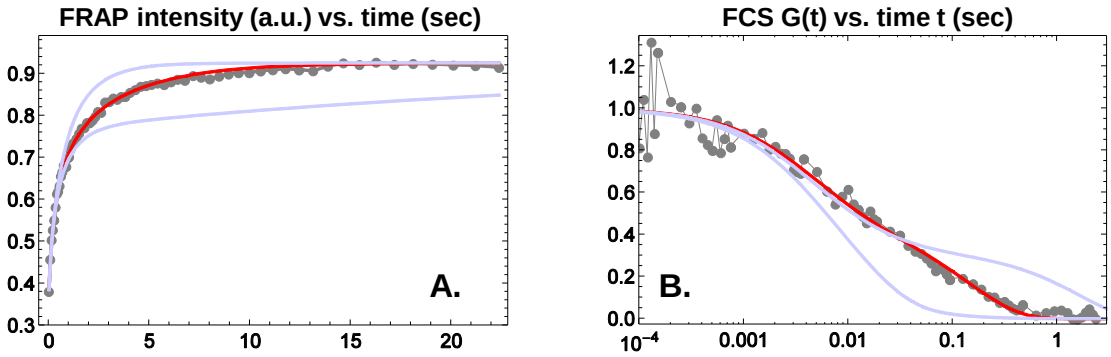

FIGURE S2. Sensitivity of FRAP and FCS single cell measurements: When single-cell **(A)** FRAP and **(B)** FCS data (gray) are fit (red curves), the fitted diffusion coefficients and bound fractions agree, but the fitted residence times disagree by over an order of magnitude. The bounding curves in light blue show how the FRAP and FCS fits would change if residence times were increased/decreased by an order of magnitude (leaving the diffusion coefficients and bound fractions fixed). Thus the procedures are sensitive enough to detect order of magnitude changes in residence times.

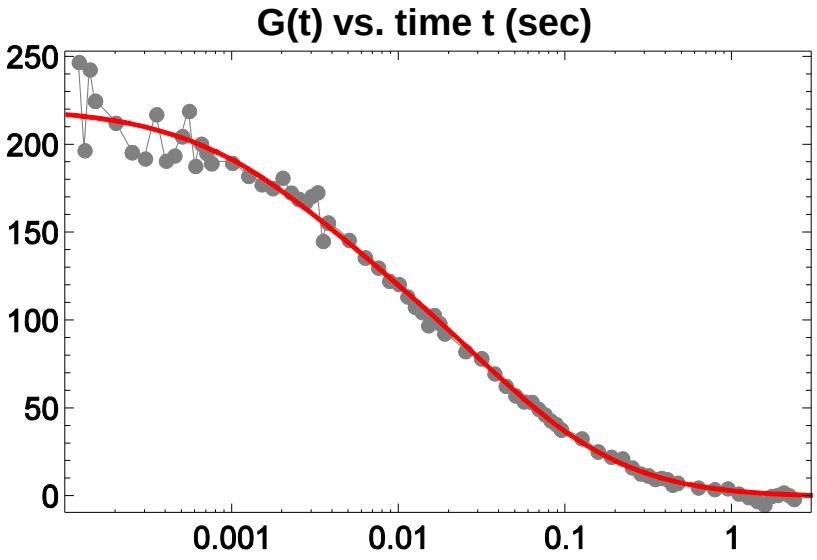

FIGURE S3. Fitting GFP-GR to a two-component diffusion model: A sample fit of the two-photon FCS data for GFP-GR to a two-component diffusion model (with diffusion coefficients D_{fast} and D_{slow}) rather than a reaction-diffusion model. This yielded $D_{fast} = 5.9 \pm 1.7$ μm^2/s and $D_{slow} = 0.36 \pm 0.06$ μm^2/s, in good agreement with estimates from an earlier study (10) that also used a two component diffusion model to fit GFP-GR.

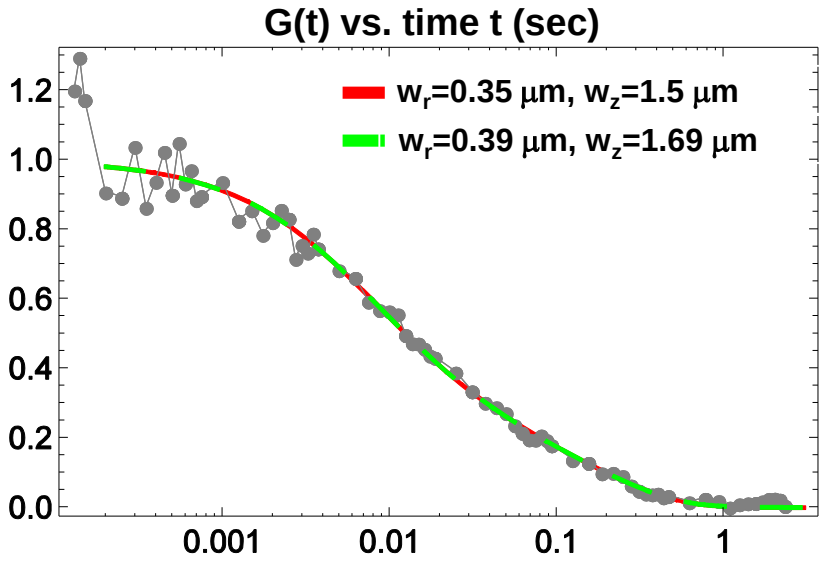

FIGURE S4. FCS re-calibration does not significantly alter fitted binding times: Depending on the value of the diffusion coefficient of Alexa 488 used for calibration (either 196 $\mu m^2/s$ (1) or 435 $\mu m^2/s$ (11)), the two-photon FCS focal volume changes from w_r=0.35 and w_z=1.5 (red) to w_r=0.39 and w_z=1.69 (green). In either case, the FCS data for GFP-GR can be well fit to yield estimates for the diffusion coefficient D, the bound fraction B, and the binding residence time t_r. Using the smaller focal volume (red) yields D=1.85 $\mu m^2/s$, B=0.21, and t_r=0.21 s. Using the larger focal volume yields D=2.36 $\mu m^2/s$, B=0.21, and t_r=0.21 s. As this example illustrates, regardless of which value is chosen, the fitted bound fractions and binding residence times remain virtually unchanged. Only the diffusion coefficient changes significantly (from D=2.51 ± 0.64 $\mu m^2/s$ to D=3.16 ± 0.75 $\mu m^2/s$).

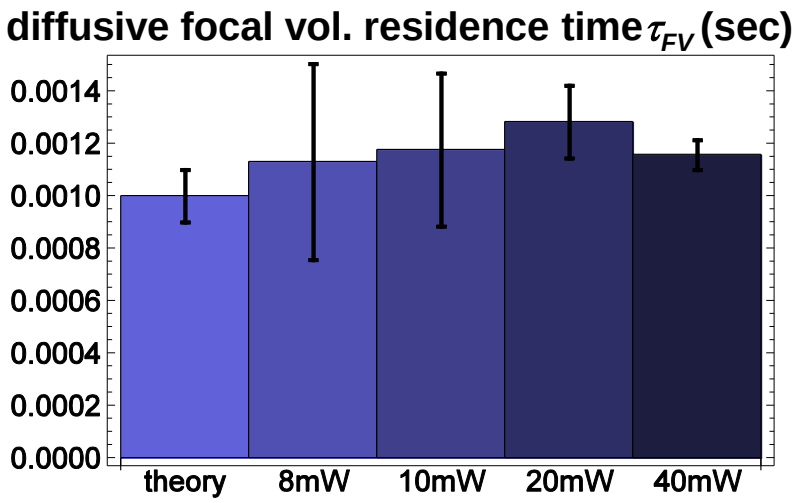

FIGURE S5. Fast molecules do not photobleach significantly: We used two-photon FCS to measure the focal volume residence time τ_{FV} of unconjugated GFP in PBS at 23 ± 2 °C. Regardless of the laser power used, fits agreed with theoretical expectations (see Table S1).

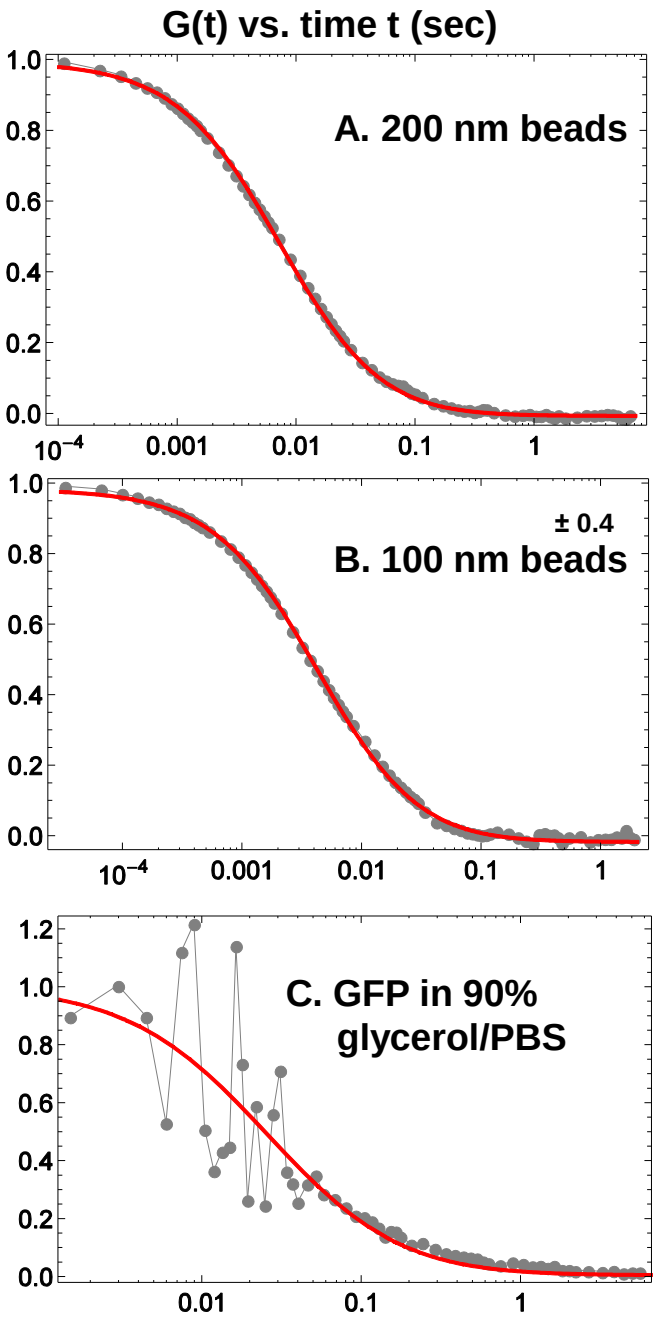

FIGURE S6. Testing the TICS procedure in solution: TICS was used to measure the diffusion coefficients *D* of **(A)** 100 nm and **(B)** 200 nm diameter fluorescent beads (FluoSpheres, Molecular Probes) in water at 37 ± 2 °C. Fits to the temporal autocorrelation G(t) of data yielded $D = 3.25 \pm 0.2$ μm^2/s for 200 nm beads and $D = 5.75 \pm 0.4$ μm^2/s for 100 nm beads, in agreement with theoretical expectations (see Table S1). (C) To test the photobleach correction, TICS was used to measure the diffusion coefficient of unconjugated GFP in a 90% glycerol/PBS solution at 37 ± 0.2 °C. Fits yielded $D = 1.26 \pm 0.4$ μm^2/s, in agreement with theoretical predictions (see Table S1).

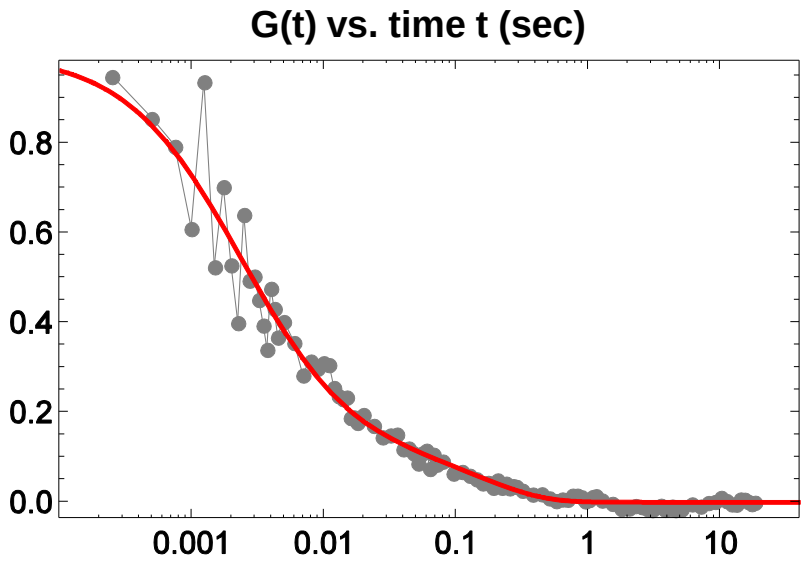

FIGURE S7. TICS on VBP-B-ZIP: TICS was used to measure the diffusion coefficient *D*, bound fraction *B*, and binding residence time t_r of VBP-B-ZIP. Fits to the temporal autocorrelation G(t) of data yielded $D = 8.2 \pm 1.9$ μm^2/s, $B = 0.13 \pm 0.10$, and $t_r = 0.27 \pm 0.13$ s.

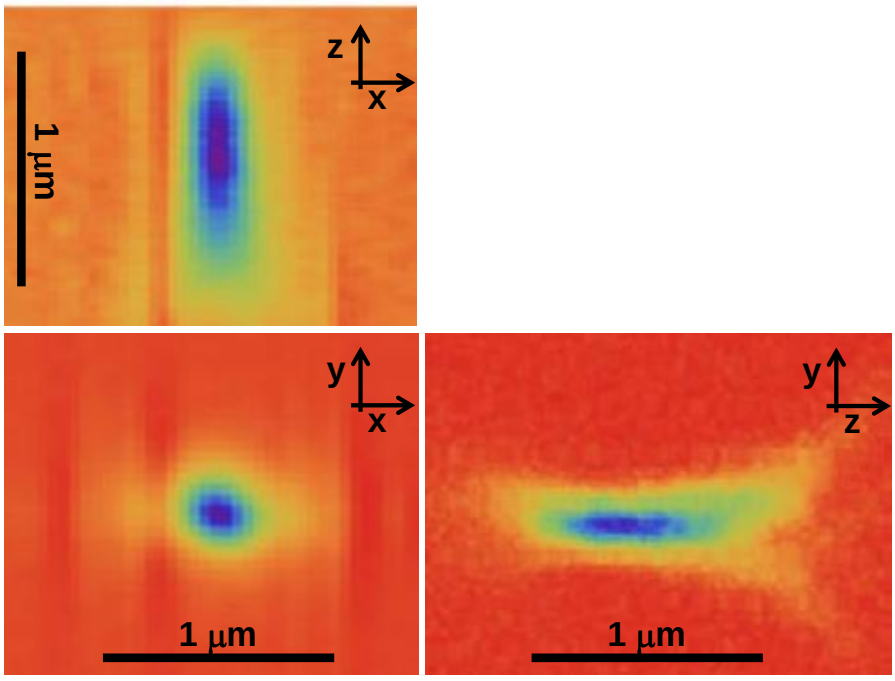

FIGURE S8. Measuring the Zeiss Live PSF: To measure the point spread function (PSF) of the Zeiss Live microscope, 3D image stacks from 100 nm beads (Fluorospheres, Molecular Probes) were acquired and fit with a 3D Gaussian [proportional to $\exp(-2x^2/w_x^2)\exp(-2y^2/w_y^2)\exp(-2z^2/w_z^2)$]. XZ, XY, and YZ cross sections from a sample 3D stack are shown. Good fits were obtained with $w_x = 0.3 \pm 0.13$ μm, $w_y = 0.25 \pm 0.09$ μm, and $w_z = 0.90 \pm 0.20$ μm. Due to the line excitation, the PSF is spread slightly more in the X direction than in the Y direction, so $w_x > w_y$ (4).